Available online at www.sciencedirect.com
SCIENCE DIRECT®
ELSEVIER
Palaeogeography, Palaeoclimatology, Palaeoecology 236 (2006) 20–38
PALAEO
www.elsevier.com/locate/palaeo

High resolution characterization of the Asian Monsoon between 146,000 and 99,000 years B.P. from Dongge Cave, China and global correlation of events surrounding Termination II

Megan J. Kelly [a,*], R. Lawrence Edwards [a], Hai Cheng [a], Daoxian Yuan [b], Yanjun Cai [c], Meiliang Zhang [b], Yushi Lin [b], Zhisheng An [c]

[a] *Department of Geology and Geophysics, University of Minnesota, MN 55455, USA*
[b] *Karst Dynamics Laboratory, The Ministry of Land and Resources, 40 Qixing Road, Guilin 541004, China*
[c] *State Key Lab of Loess and Quaternary Geology, Institute of Earth Environment, Chinese Academy of Sciences, Xi'an 710075, China*

Received 30 September 2004; accepted 11 November 2005

Abstract

Speleothem samples from Hulu (eastern China, 32°30′N, 119°10′E) and Dongge (southern China, 25°17′N, 108°5′E) Caves provide a nearly continuous record of the Asian monsoon over the last 160 ka [Wang, Y.J., Cheng, H., Edwards, R.L., An, Z.S., Wu, J.Y., Shen, C.-C., Dorale, J.A., 2001. A high-resolution absolute-dated Late Pleistocene monsoon record from Hulu Cave, China. Science 294, 2345–2348; Yuan, D., Cheng, H., Edwards, R.L., Dykoski, C.A., Kelly, M.J., Zhang, M., Qing, J., Lin, Y., Wang, Y., Wu, J., Dorale, J.A., An, Z., Cai, Y., 2004. Timing, duration, and transitions of the last interglacial Asian Monsoon. Science 304, 575–578]. We have obtained higher resolution data in the interval between ~99 and 146 ka B.P., providing a detailed account of $\delta^{18}O$ variations over most of MIS 5 and the latter portion of MIS 6. Precise ^{230}Th dating has replicated the chronology of the samples within error. The higher resolution data set confirms the timing of Asian Monsoon Termination II (the midpoint of the negative shift in $\delta^{18}O$ marking the onset of the Last Interglacial Asian Monsoon), placing it at 129.0±0.9 ka B.P. The bulk of this transition (~1.7‰) took place within approximately 70 years, with the total range of the transition being ~3‰. The most abrupt portion of the shift in $\delta^{18}O$ values (~1.1‰) marking the end of the Last Interglacial Asian Monsoon occurred in ~120 years, the midpoint of which is 120.7±1.0 ka B.P. The Dongge Cave monsoon $\delta^{18}O$ record over late MIS 6 exhibits a series of sub-orbital millennial-scale climate shifts that average 1.3‰ in magnitude and occur on average every 1.8 ky. Abrupt shifts in $\delta^{18}O$ of up to 1‰ also occurred throughout the Last Interglacial Asian Monsoon, with periods at multi-decadal to centennial timescales. Similar to the amplitude and periodicities of events found by Dykoski et al. [Dykoski, C.A., Edwards, R.L., Cheng, H., Yuan, D., Cai, Y., Zhang, M., Lin, Y., An, Z., Revenaugh, J., 2005. A high resolution, absolute-dated Holocene and deglacial Asian monsoon record from Dongge Cave, China. Earth and Planetary Science Letters 233, 71–86.] during the Holocene in the Dongge record, these shifts cover more than 1/2 of the amplitude of millennial-scale and multi-centennial-scale interstadial events during the Last Glacial Period [Wang, Y.J., Cheng, H., Edwards, R.L., An, Z.S., Wu, J.Y., Shen, C.-C., Dorale, J.A., 2001. A high-resolution absolute-dated Late Pleistocene monsoon record from Hulu Cave, China. Science 294, 2345–2348], and millennial-scale and multi-centennial-scale interstadial events during the Penultimate Glacial Period in China (this study). Abrupt decadal to millennial-scale climate events therefore appear to be a general feature of both glacial and interglacial climate. We demonstrate that monsoon intensity correlates well with atmospheric CH_4 concentrations over the transition into the Bølling-Allerød, the Bølling-Allerød, and the Younger Dryas. In addition, we correlate an abrupt jump in CH_4 concentration with Asian Monsoon Termination

* Corresponding author. Tel.: +1 612 626 7663; fax: +1 612 625 3819.
E-mail address: kell0738@umn.edu (M.J. Kelly).

0031-0182/$ - see front matter
doi:10.1016/j.palaeo.2005.11.042

II. On the basis of this correlation, we conclude that the rise in atmospheric CO_2, Antarctic warming, and the gradual portion of the rise in CH_4 around Termination II occur within our "Weak Monsoon Interval" (WMI), an extended interval of heavy $\delta^{18}O$ between 135.5±1.0 and 129.0±1.0 ka B.P., prior to Asian Monsoon Termination II and Northern Hemisphere warming. Antarctic warming over the millennia immediately preceding abrupt northern warming may result from the "bipolar seesaw" mechanism. As such warming (albeit to a smaller extent) also preceded Asian Monsoon Termination I, the "bipolar seesaw" mechanism may play a critical role in glacial terminations.

Keywords: Speleothems; Monsoon; U–Th dating; Oxygen isotopes; Termination II

1. Introduction

The Asian Monsoon is an important component of the global climate system, for it has been linked to climate in the high northern latitudes, the equatorial ocean, and the southern hemisphere. For the last 2.5 Ma, global climate has been dominated by glacial–interglacial cycles. Continental responses to these cycles, including the monsoon, are important to the study of global circulation patterns and climate linkages. Speleothem calcite is one of the few terrestrial climate proxies with potential for continuous deposition over long periods of time, providing a detailed record of oxygen isotopic signatures for the duration of speleothem growth. If the calcite is formed under equilibrium conditions, oxygen isotope ratios recorded in speleothems from China may be considered a proxy for the $\delta^{18}O$ of monsoon precipitation. Oxygen isotopic data from speleothems combined with absolute ages determined by ^{230}Th dating has the potential to provide a high-resolution record of monsoon variability on both orbital and sub-orbital timescales.

Climate during the most recent glacial cycle has been extensively studied, but many questions remain regarding the Last Interglacial and the Penultimate Glacial periods. The Last Interglacial (MIS 5e) climate is particularly important because it may be considered an analog to the present warm period. The sequence of events surrounding glacial terminations is a key issue in understanding the connections between different areas of the globe. In addition, more precise studies of the Penultimate Glacial (MIS 6) as it compares to the well documented record of the Last Glacial Period will provide further insight on the present theory on glacial climate.

Previous work has demonstrated a strong correlation between the oxygen isotope record of speleothems from Hulu Cave, China, and the GISP2 $\delta^{18}O$ record between 11 and 75 ka B.P. (Wang et al., 2001). This includes the Younger Dryas event and Bølling-Allerød (B/A) transition, as well as millennial-scale climatic variations. Greenland Interstadial (GIS) events during the Last Glacial Period correspond to episodes of more negative monsoon $\delta^{18}O$ values at Hulu Cave. In addition, heavy excursions in the Hulu $\delta^{18}O$ record have been linked to Heinrich events 1–6 during the Last Glacial Period.

Yuan et al. (2004) presented the first stable isotope work on speleothems from Dongge Cave, China. They demonstrated a similar connection to high northern latitude climate as well as Northern Hemisphere insolation. To further our understanding of sub-orbital climate events we have increased the resolution of a portion of this record from 146 to 99 ka B.P. A higher resolution Asian Monsoon record over this time period has enabled more accurate correlations between global and regional climate records, and facilitates the understanding of forcing mechanisms and lead/lag relationships associated with insolation changes, ice volume, sea level, and terrestrial responses to these changes.

2. Site description

Dongge Cave is located in the Guizhou Province of southern China (25°17′N, 108°5′E), 680 m above sea level (Fig. 1). Our study focuses on stalagmites D3 and D4, which were located 100 m below the surface, and 300 and 500 m from the cave entrance, respectively. Modern climatic information from this area has previously been reported by Yuan et al. (2004). The mean annual temperature within the cave is 15.6 °C. Average annual rainfall is 1753 mm, 80% of which falls during the summer monsoon (May–October). Oxygen isotopic data of meteoric precipitation from nearby Guiyang, China (26.35°N/106.43°E) exhibits a seasonal pattern characteristic of a monsoon climate (IAEA/WMO, 2001). Despite generally higher temperatures during the summer months, weighted monthly $\delta^{18}O$

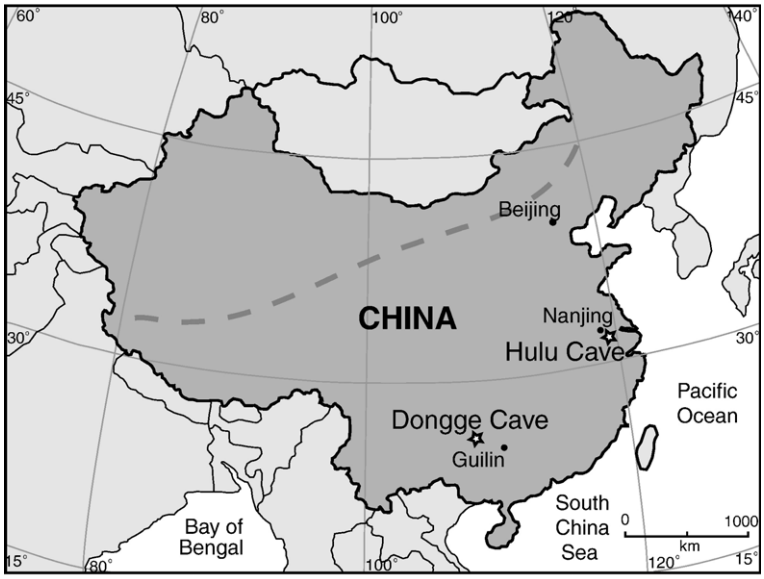

Fig. 1. Map of China and surrounding areas, including the locations of Dongge (southern China, 25°17′N, 108°5′E) and Hulu (eastern China, 32°30′ N, 119°10′E) Caves. Dashed line illustrates the approximate northern extent of the Asian summer monsoon.

values are lighter (average ~− 9.6‰) than those during the winter months (average ~− 4.6‰).

3. Methods

Samples from speleothems D3 and D4 were prepared for ^{230}Th dating following procedures similar to those described by Edwards et al. (1987) and Dorale et al. (2005). Approximately 100–200 mg of calcite powder was drilled out from along a particular growth horizon. Samples were dissolved in nitric acid, spiked with a mixed ^{233}U–^{236}U–^{229}Th tracer, and dried down. The samples were then re-dissolved in weak hydrochloric acid and a drop of FeCl solution was added. Iron, uranium, and thorium were co-precipitated with the drop-wise addition of NH_4OH. Samples were then centrifuged in order to isolate the solid fraction. Uranium and thorium were separated from one another by running the sample through columns containing anion resin. Finally, the samples were dried down and dissolved in a weak nitric acid solution to prepare them for analysis. For D4, uranium concentrations are ~300–600 ppb so that each sub-sample (of 200 mg) contains about 60–120 ng of uranium and ~1 pg of ^{230}Th. Uranium concentrations are slightly higher in D3 (~500–1200 ppb), so smaller sub-samples of ~100 mg provided approximately the same amount of uranium and ^{230}Th. Radiometric ages of speleothem calcite can be obtained efficiently with the application of U-series dating techniques on inductively coupled plasma mass spectrometers (ICP-MS) (Stirling et al., 2000; Shen et al., 2002). ICP-MS analyses of speleothems D3 and D4 from Dongge Cave were made at the Minnesota Isotope Laboratory on a Finnigan-MAT Element equipped with a double-focusing sector-field magnet in reversed Nier-Johnson geometry and a single MasCom multiplier. 2σ analytical errors associated with the ^{230}Th dates vary based on the age of the sample, and are approximately 500–1000 years for speleothems that were formed during the Last Interglacial and Penultimate Glacial periods (Dorale et al., 2005).

Oxygen and carbon isotopes were analyzed at the Institute of Earth Environment, Xi'an, China and the Minnesota Isotope Laboratory, Minneapolis, USA. At both locations, measurements were made on a Finnigan-MAT 252 mass spectrometer fitted with a Kiel Carbonate Device III. Samples were calibrated against the NBS-19 standard and are reported as δ^{18}O and δ^{13}C (‰) relative to the Vienna Pee Dee Belemnite (VPDB) standard. Duplicates were analyzed every 10 to 20 samples, all of which replicated within 0.15‰ for oxygen and 0.20 ‰ for carbon.

4. δ^{18}O—climate interpretation

Speleothem δ^{18}O values can be interpreted in terms of climate only if the system has remained closed from water/rock interactions and/or kinetic processes. There are several ways to ensure that kinetic fractionation was

not a factor during calcite deposition. The traditional Hendy Criteria for isotopic equilibrium state that $\delta^{18}O$ should be constant along a single growth horizon, and that $\delta^{13}C$ and $\delta^{18}O$ should not covary down the length of the growth axis (Hendy, 1971). In addition, Hendy (1971) noted that a strong positive correlation between carbon and oxygen isotopic values may indicate that kinetic processes have taken place. However, Dorale et al. (1998) demonstrate that a positive correlation could also result from a true climate signal relating vegetation changes to changes in climate.

Replication is another rigorous test for isotopic equilibrium (Dorale et al., 1998). This involves the comparison of two or more speleothem records from different caves or different locations within the same cave that grew during an overlapping time period. Speleothems collected from different locations have most likely experienced variable growth conditions, such as flow path, drip rates, CO_2 partial pressures, residence time, concentration of solutes, and degassing history. Considering the number of variables involved, it is unlikely that different speleothems would exhibit matching isotopic records if kinetic processes had taken place (Dorale et al., 1998). Therefore, duplicated records can be considered an accurate measure of the true climate signal.

It has previously been established that the $\delta^{18}O$ record from speleothem D4 from Dongge Cave and speleothem H82 from Hulu Cave replicate one another over a younger time interval (Yuan et al., 2004). In addition, $\delta^{18}O$ of speleothems D3 and D4, both from Dongge Cave, generally replicate one another across the overlapping growth period (Figs. 2 and 3 in Yuan et al., 2004). This suggests that the Dongge Cave speleothem $\delta^{18}O$ record is an accurate reflection of local and regional climate. Correlation between carbon and oxygen in samples D3 and D4 is generally very low, with r^2 values for both samples ~ 0.03. The strongest positive correlation occurs during the Last Interglacial Period in both D3 ($r^2 \sim 0.4$) and D4 ($r^2 \sim 0.6$). As long-term correlations are poor, and our records generally replicate (see above), we assume that the high r^2 values during the Last Interglacial are likely due to a true environmental correlation as discussed above. Thus, it appears that water/rock interactions and kinetic fractionation have not affected the Dongge Cave speleothem $\delta^{18}O$ values. The $\delta^{18}O$ of calcite is therefore a reflection of temperature and/or the $\delta^{18}O$ of meteoric precipitation. Speleothems D3 and D4 from Dongge Cave show glacial–interglacial $\delta^{18}O$ amplitudes of 4–5‰ (this study). Due to the small temperature-dependent fractionation between calcite and water (−0.23‰/°C (Friedman and O'Neil, 1977)), $\delta^{18}O$ variations of this magnitude must primarily be controlled by changes in the $\delta^{18}O$ of precipitation.

The question then becomes, how does one interpret $\delta^{18}O$ in terms of climate? Global patterns in the $\delta^{18}O$ of precipitation ($\delta^{18}O_p$) are mainly a reflection of the amount of moisture lost from an air mass as it moves away from the source region (Dansgaard, 1964). This process can be described by a Rayleigh condensation model, where the condensate is immediately removed and isolated from the air mass after formation (see below). As a result of this process, correlations have been observed at different geographical locations between $\delta^{18}O_p$ and temperature ("temperature effect"), and $\delta^{18}O_p$ and amount of precipitation ("amount effect"). In general, regions where the mean annual temperature (MAT) is lower than 10 °C exhibit a strong, positive correlation between $\delta^{18}O_p$ and temperature (Jouzel et al., 1994). Conversely, in tropical regions the $\delta^{18}O_p$–temperature correlation is weak, and $\delta^{18}O_p$ instead appears to be a function of the strong inverse relationship between $\delta^{18}O_p$ and precipitation amount (Rozanski et al., 1993).

In an empirical study, Johnson and Ingram (2004) examined in detail the relationships between $\delta^{18}O_p$, temperature, and precipitation in China using modern climate data from 10 sites in the Global Network of Precipitation database (GNIP). For each site, they have regressed $\delta^{18}O_p$ with temperature and precipitation in order to estimate values of $d\delta^{18}O_p/dP$ and $d\delta^{18}O_p/dT$. Their results demonstrate that in southern China, $\delta^{18}O_p$ is most strongly influenced by the amount of precipitation. In addition, their multiple regression equations constitute an empirical model that can predict $\delta^{18}O_p$ in modern day China. However, when one tries to use this model to reconstruct past changes in $\delta^{18}O$ of precipitation based on our data, we find that an extremely large change in precipitation amount, greater than 95%, is required to account for the 4‰ to 5‰ glacial–interglacial amplitude of our record. Though the Johnson and Ingram (2004) model is able to represent the modern relationships between $\delta^{18}O_p$, temperature, and amount of precipitation across China, we find that changes observed in the past cannot be predicted on the basis of these modern relationships. This demonstrates that fundamental changes in circulation occurred in the past. These changes shifted the relationship between $\delta^{18}O$ and precipitation in a different fashion than the relationship observed in the modern data.

Because we are not able to accurately extrapolate to the past based on modern empirical relationships, we must search for other ways to interpret our data. Wang et

al. (2001) found a general anti-correlation between $\delta^{18}O$ values at Hulu Cave and those in Greenland ice over the last glacial cycle. They proposed that long-term $\delta^{18}O$ variations at Hulu Cave are related to the strong seasonality of $\delta^{18}O$ of precipitation. According to this interpretation, variations in $\delta^{18}O$ values at Hulu Cave result from changes in the ratio of summer (characteristically more negative) vs. winter (characteristically more positive) precipitation. During a strong summer monsoon, a larger percentage of the annual precipitation budget would come from summer precipitation, resulting in more negative $\delta^{18}O$ values. Negative shifts in Hulu Cave $\delta^{18}O$ values can therefore be related to periods of high summer monsoon intensity, and vice versa. This is a reasonable interpretation for our Dongge Cave $\delta^{18}O$ record.

Alternatively, one could interpret the $\delta^{18}O$ pattern in terms of a simple Rayleigh model. Yuan et al. (2004) pursued this interpretation because the Wang et al. (2001) interpretation is not applicable to locations outside of China. For instance, speleothems from Israel (Bar-Matthews et al., 2003) and Venezuela (Gomez et al., 2003) demonstrate a similar anti-correlation with Greenland ice despite having different modern seasonal relationships. Yuan et al. (2004) used the following Rayleigh fractionation equation (modified from Criss, 1999),

$$(1000 + \delta_p)/(1000 + \delta_{sw}) = f^{(\alpha-1)},\ \alpha = 1.0094,$$

where δ_p is the $\delta^{18}O$ of precipitation, δ_{sw} is the $\delta^{18}O$ of the source water, f is the fraction of water vapor remaining, and α is the fractionation factor between liquid water and vapor. According to this model, $\delta^{18}O_p$ in the Hulu/Dongge Cave region can be considered a measure of the fraction of water vapor removed from the air masses between the moisture source region (tropical Indo-Pacific) and southeastern China. The amount of precipitation integrated from the source region to the Hulu/Dongge region would therefore be lower during glacial periods than interglacial periods, indicating that drier conditions existed over southern China during glacial periods. In detail, the integrated precipitation values during glacial times would be ~65% of values during the mid-Holocene/Last Interglacial (Yuan et al., 2004). The Wang et al. (2001) and Yuan et al. (2004) explanations are qualitatively similar and are both viable interpretations, relating changes in the $\delta^{18}O$ of precipitation in China to summer monsoon intensity. This has significant implications for determining the connections that exist between different regional and global climate records.

5. Results

A total of thirty-six new ^{230}Th dates were determined for D3 and D4, replicating the original timescale of Yuan et al. (2004) within error (Table 1). All ages were corrected for initial ^{230}Th using the value $(7\pm5)\times10^{-6}$, a value calculated from the initial $^{230}Th/^{232}Th$ ratios required to place several samples with anomalously high ^{232}Th values in correct stratigraphic order (Yuan et al., 2004; Dykoski et al., 2005). Nineteen dates were obtained from sample D4, which cover the older portion of the record between 125.4±0.8 and 145.9±1.3 ka B.P. A group of 4 sub-samples, D4N4, D4N5, D4N6, and D4B1, were all very close in depth and their ages were essentially the same within the given 2σ error. These samples were considered replicates and average ages and depths were used to develop the D4 timescale. A similar procedure was followed for a group of three older sub-samples D4A1, D4N7, and D4A4. In both cases, the averaged values lie within the error limits of the points involved (see Fig. 2a). Over the dated time interval, the average growth rate for sample D4 was 28 μm/year and varied between 7 and 90 μm/year as shown in Fig. 2a. Over most of this time period there are no obvious hiatuses in growth. However, the growth rate does slow down significantly during the second half of MIS 5e, and it is possible that there are one or more short duration hiatuses in the portion of D4 younger than 125 ka B.P. Seventeen new ^{230}Th ages were obtained from speleothem D3 (which includes 3 duplicate analyses) between 99.7±0.8 ka and 125.3±1.2 ka (Table 1, Fig. 2b). Replicate sub-samples D3D4a and D3D4b were simply averaged, while the other two replicate pairs, D3D2a/D3D2b and D3B3a/D3B3b, were grouped with D3D3 and D3B1, respectively, and averaged as for the D4 sub-samples described above. Across this time interval, there do not appear to be any hiatuses in growth. D3 had a slightly faster average growth rate than D4, 56 μm/year, varying between 22 μm/year and 170 μm/year (Fig. 2b, lower panel).

A number of previous speleothem studies have demonstrated a correlation between growth rate and changes in precipitation (Genty and Quinif, 1996; Musgrove et al., 2001; Bard et al., 2002), though we do not see such a correlation in our Dongge Cave record between 99 and 146 ka B.P. Because of the complex nature of groundwater flow through the vadose zone, there may well be no correlation between speleothem growth rate and precipitation amount (Baker et al., 1997). In addition, several other factors are shown to influence growth rate, such as drip rate, Ca concentrations of the drip water, and temperature, which can make

Table 1
^{230}Th dating results for stalagmites D3 and D4 by ICP-MS analysis

Sample number	Depth (cm)	^{238}U (ppb)	^{232}Th (ppt)[a]	δ^{234}U (measured)	^{230}Th/^{238}U (activity)	^{230}Th age (ka; uncorrected)	^{230}Th age (ka; corrected)	$\delta^{234}U_{Initial}$ (corrected)	Growth rate[b] (μm/year)
D3									
D3F1	35.0	648±1.0	3865±47	−212.5±1.4	0.4560±0.0019	100.2±0.8	99.7±0.8	−281.8±2.0	
D3F2	47.3	657±1.0	260±32	−225.4±1.4	0.4484±0.0017	100.6±0.7	100.6±0.7	−299.4±1.9	153
D3E1	62.1	797±1.4	4549±44	−192.3±1.3	0.4844±0.0021	105.7±0.9	105.3±0.9	−259.3±1.9	31
D3D1	78.7	804±2.3	352±40	−187.3±1.6	0.5028±0.0021	111.6±1.0	111.6±1.0	−256.8±2.3	27
D3D4a[c]	93.3	1098±2.1	610±45	−190.0±1.4	0.5041±0.0019	112.9±0.9	112.9±0.9	−261.4±2.0	85
D3D4b[c]	93.3	1091±2.0	597±40	−190.1±1.4	0.5058±0.0019	113.7±0.9	113.6±0.9	−262.2±2.0	–
D3D5	103.4	784±1.3	159±44	−195.2±1.4	0.5038±0.0020	114.4±0.9	114.4±0.9	−269.7±2.0	88
D3D2a[c, d]	109.4	1124±2.2	420±46	−200.1±1.8	0.5061±0.0022	117.0±1.1	117.0±1.1	−278.4±2.7	22
D3D2b[c, d]	109.4	1129±3.8	570±61	−201.8±2.6	0.5070±0.0024	118.0±1.4	118.0±1.4	−281.6±3.8	–
D3D3[d]	111.1	944±1.7	231±41	−208.7±1.5	0.4999±0.0019	117.2±1.0	117.2±1.0	−290.6±2.2	–
D3C1N	122.3	1279±2.2	563±41	−196.0±1.2	0.5134±0.0020	118.9±1.0	118.9±1.0	−274.2±1.9	82
D3B2	139.8	1101±1.9	524±48	−206.5±1.3	0.5090±0.0020	120.6±1.0	120.5±1.0	−290.3±2.0	104
D3B3a[c, d]	148.5	1006±1.9	1760±47	−194.1±1.3	0.5219±0.0021	122.1±1.1	121.9±1.1	−274.1±2.1	59
D3B3b[c, d]	148.5	1003±1.9	2059±48	−195.0±1.4	0.5240±0.0024	123.4±1.2	123.2±1.3	−276.3±2.2	–
D3B1[d]	156.3	534±0.9	4139±52	−190.9±1.3	0.5256±0.0019	122.6±1.0	122.1±1.0	−269.7±2.0	–
D3A2	161.0	1016±2.0	466±41	−198.4±1.5	0.5234±0.0020	124.4±1.1	124.3±1.1	−282.0±2.4	52
D3A1	177.7	954±1.8	1887±43	−192.8±1.5	0.5301±0.0023	125.4±1.2	125.3±1.2	−274.8±2.3	170
D4									
D4D1	243.9	516±0.6	2467±23	−61.0±1.1	0.6345±0.0020	125.5±.8	125.3±0.8	−87.0±1.6	
D4D2	253.4	548±0.8	3301±24	−67.8±1.3	0.6357±0.0023	128.1±1.0	127.8±1.0	−97.3±1.9	38
D4C1	257.8	618±0.8	82±22	−39.7±1.2	0.6592±0.0019	128.3±.79	128.3±0.8	−57.1±1.7	86
D4C2	261.3	358±0.6	67±23	−38.2±1.8	0.6626±0.0023	129.1±1.0	129.1±1.0	−55.1±2.7	43
D4N1	263.5	284±0.4	249±11	−14.2±1.5	0.6844±0.0035	130.0±1.4	129.9±1.4	−20.4±2.2	27
D4C3	268.2	310±0.4	648±21	−12.0±1.6	0.6886±0.0024	130.9±1.0	130.8±1.0	−17.3±2.3	53
D4B2	271.8	347±0.5	759±24	−10.6±1.5	0.6948±0.0024	132.8±1.0	132.7±1.0	−15.4±2.2	19
D4N2	275.0	357±0.4	330±11	−18.7±1.3	0.6939±0.0024	135.0±1.0	134.9±1.0	−27.4±1.9	14
D4N3	276.0	348±0.4	365±11	−34.7±1.2	0.6832±0.0023	136.0±1.0	136.0±1.0	−51.0±1.8	10
D4N4[d]	281.0	352±0.4	371±11	−16.5±1.3	0.7012±0.0023	137.1±1.0	137.0±1.0	−24.2±1.9	90
D4N5[d]	282.1	352±0.4	577±11	−30.8±1.3	0.6881±0.0023	136.6±1.0	136.6±1.0	−45.3±1.9	–
D4N6[d]	282.5	309±0.4	137±11	−47.1±1.3	0.6750±0.0024	136.9±1.1	136.8±1.1	−69.4±1.9	–
D4B1[d]	283.1	496±0.7	988±22	−36.5±1.5	0.6822±0.0022	136.3±1.0	136.2±1.0	−53.7±2.1	–
D4A1[d]	287.8	341±0.5	953±21	−29.8±1.5	0.6992±0.0031	140.9±1.4	140.8±1.4	−44.3±2.2	24
D4N8[d]	288.7	351±0.4	3163±13	−27.8±1.4	0.6948±0.0023	138.3±1.0	137.9±1.1	−41.1±2.0	–
D4A4[d]	289.0	402±0.6	573±25	−32.7±1.4	0.6930±0.0029	139.3±1.3	139.2±1.3	−48.5±2.1	–
D4N7	290.3	253±0.3	10138±25	−36.2±1.3	0.7012±0.0027	144.0±1.3	142.0±1.4	−54.4±2.0	7
D4A2	294.2	381±0.5	5218±28	−34.0±1.5	0.7019±0.0035	143.9±1.6	143.3±1.6	−51.0±2.2	31
D4A3	301.0	532±0.8	2740±24	−44.0±1.5	0.6990±0.0027	146.2±1.3	145.9±1.3	−66.5±2.2	26

Errors are 2σ analytical errors.
[a] ppt=parts per trillion.
[b] Refers to the growth rate between dated sub-sample and immediately younger sub-sample.
[c] a and b indicate duplicate analyses.
[d] Indicates groups of samples that were averaged for the age interpolation (as seen in Fig. 2). Decay constant values are $\lambda_{230}=9.1577\times10^{-6}$ year^{-1}, $\lambda_{234}=2.8263\times10^{-6}$ year^{-1}, $\lambda_{238}=1.55125\times10^{-10}$ year^{-1}. Corrected ^{230}Th ages assume the initial ^{230}Th/^{232}Th atomic ratio of $(7\pm5)\times10^{-6}$.

direct climatic interpretation fairly complicated (Dreybrodt, 1980; Baker et al., 1997, 1998).

We do, however, see a negative correlation between growth rate and initial δ^{234}U in both D3 and D4, a relationship that has also been observed in several speleothem records (Fig. 3; Kaufman et al., 1998; Hellstrom and McCulloch, 2000). Initial δ^{234}U ratios of speleothem calcite reflect that of the drip water. Radiogenic production of ^{234}U by α-emission leads to uranium disequilibrium via recoil displacement of ^{234}U directly into the liquid phase, or by preferential leaching of ^{234}U into groundwater as a result of recoil damage to the chemical bonds holding the ^{234}U atom in place (Osmond, 1980). At Dongge Cave, δ^{234}U values are negative, ranging from − 299‰ to − 257‰ in D3, and from − 97‰ to − 15‰ in D4 (Table 1). δ^{234}U values in

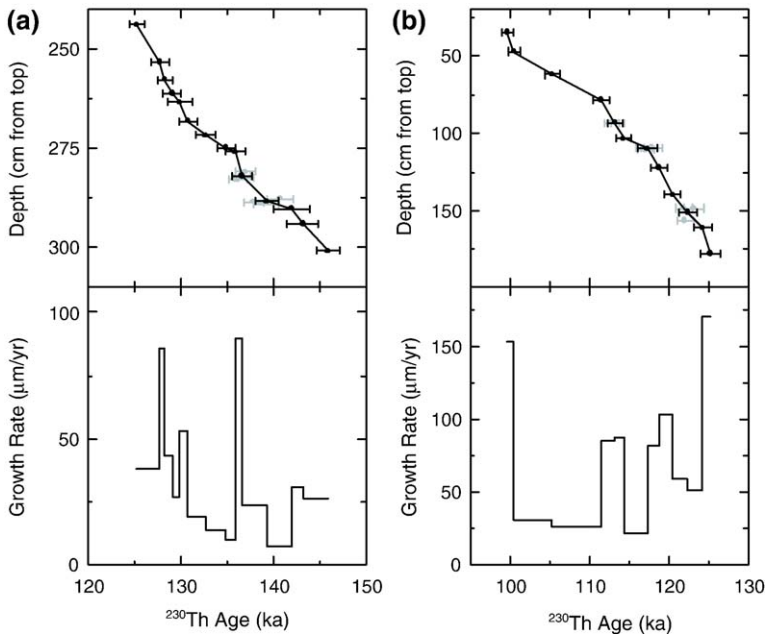

Fig. 2. Depth (upper panels) and growth rate (lower panels) vs. age for stalagmites (a) D4 and (b) D3. Error bars indicate 2σ analytical error. Replicates/overlapping samples that were averaged for the final timescale are shown in gray in the upper panels (see Table 1).

groundwater that are less than zero are considered to be unusual due to the higher mobility of ^{234}U (Osmond and Cowart, 1982). Typically, δ^{234}U values of soils are around − 100‰, though Rosholt et al. (1966) report values as low as − 416‰. One could envision low groundwater δ^{234}U values in such areas where a considerable amount of ^{234}U has previously been removed from the soil or host material.

In the Dongge Cave record, we find that initial δ^{234}U values are at their lowest when growth rate is high and vice versa (Fig. 3). Ayliffe and Veeh (1988) describe a process where the frequency and duration of wetting events control groundwater δ^{234}U values. Frequent or prolonged wet periods prevent significant ^{234}U accumulation in the soil, resulting in lower groundwater δ^{234}U values, whereas infrequent wet periods enable ^{234}U to accumulate and then be mobilized during the subsequent wetting event. Residence time, or flow rate, may also be a factor in determining the δ^{234}U of groundwater, with rapid percolation rates resulting in low δ^{234}U (Henderson et al., 1999; Hellstrom and McCulloch, 2000). Therefore, variability in the drip water δ^{234}U values appears to be closely related to the hydrology of the watershed, which is not necessarily a direct expression of precipitation amount. Low δ^{234}U ratios would likely reflect a high flux of fluid passing through the watershed, whereas higher δ^{234}U values would likely reflect slow percolation rates and/or infrequent wet periods.

More than 1600 stable isotope analyses were performed on samples D3 and D4 over the time interval between 99 and 146 ka BP (~650 from D4, ~980 from D3). Average spatial resolution of sub-samples drilled for stable isotope analysis was 0.3 mm to 0.5 cm, depending on growth rate. We established our timescale by linearly interpolating between ^{230}Th-dated points. The average temporal resolution of the oxygen data from stalagmite D3 is 27 years, though over sections with a faster growth rate the resolution is as high as 5 years. Average isotopic sampling resolution was 64 years for stalagmite D4, though again over some time intervals the resolution was much higher, between 5 and 10 years. As expected, the new high resolution oxygen data follows the general trend of the earlier data from Yuan et al. (2004), and also follows summer insolation at 25°N (Fig. 4). The overall glacial–interglacial amplitude remains approximately 5‰. However, fine scale structure is clearly visible that was previously obscured in the lower resolution data set.

Our high resolution δ^{18}O record begins at ~146 ka B.P., during the latter portion of the Penultimate Glacial Period (MIS 6). The ~700 year gap that interrupts the record is the result of a natural break in the sample that prevented isotope sampling. A large portion of the MIS 6 monsoon is characterized by abrupt shifts in δ^{18}O (Fig. 5). Negative excursions in δ^{18}O are broadly similar to peaks observed in the Last Glacial Asian Monsoon that correspond to Greenland Interstadial (GIS) events

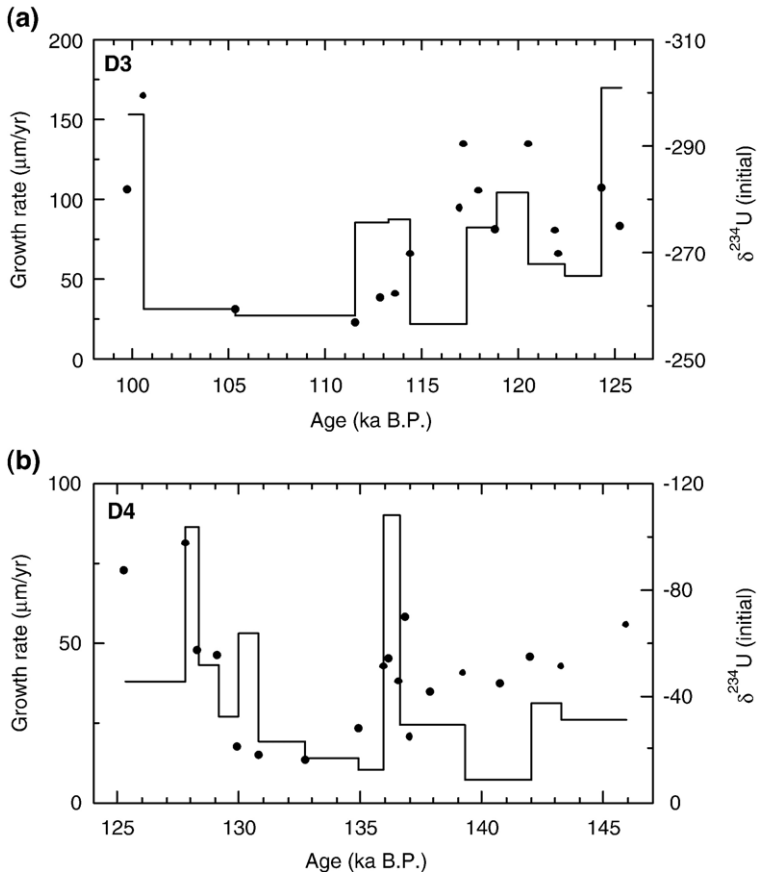

Fig. 3. Growth rate and initial δ^{234}U (see values in Table 1) vs. age for stalagmites (a) D3 and (b) D4. In general, we see a negative correlation between initial δ^{234}U and growth rate in both records. δ^{234}U appears related to the hydrology of the watershed, which may not directly reflect the amount of precipitation.

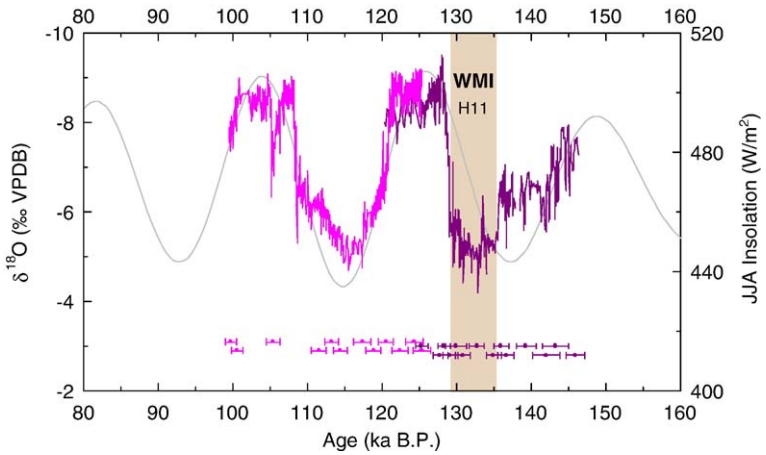

Fig. 4. New δ^{18}O time series for speleothems D3 (pink), D4 (purple), and summer insolation at 25°N (dashed line) integrated over the months of June, July, and August (Berger, 1978). Error bars are color coded by sample and indicate ^{230}Th ages and 2σ error. (For interpretation of the reference to colour in this figure legend, the reader is referred to the web version of this article.)

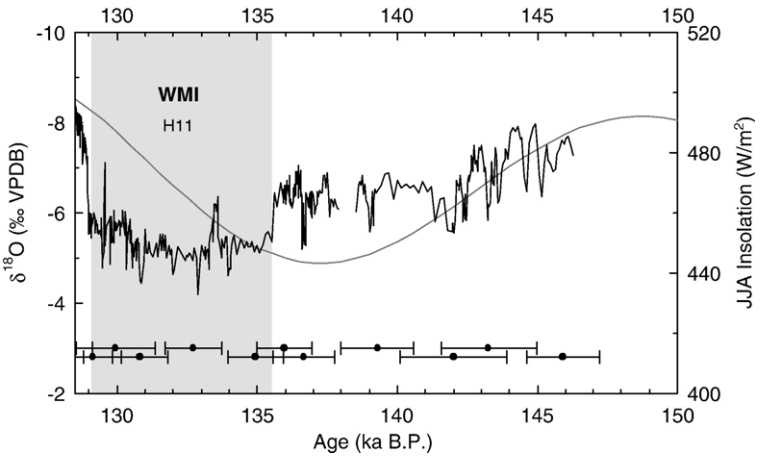

Fig. 5. $\delta^{18}O$ time series for speleothem D4 during the Penultimate Glacial Period. The Weak Monsoon Interval (WMI) occurs between 135.5±1.0 and 129.0±1.0 ka B.P., and is indicated by the vertical bar. This interval likely corresponds to H11 from North Atlantic sediment records (McManus et al., 1998). Eight multi-centennial to millennial-scale climate shifts average 1.3‰ in amplitude and occur on average every 1.8 ky.

(Wang et al., 2001). Our MIS 6 peaks average ~1.3‰ in magnitude. Approximately 8 events with an amplitude ≥1‰ occurred between 146 and 130 ka B.P. The heaviest $\delta^{18}O$ values during the latter portion of the Penultimate Glacial Period were initiated at 135.5±1.0 ka B.P., and are largely maintained for the next ~6 ky until the abrupt negative shift in $\delta^{18}O$ marking the transition into the Last Interglacial Asian Monsoon (Yuan et al., 2004). This interval is generally characterized by much less variability than seen during the earlier portions of MIS 6, with $\delta^{18}O$ values remaining around − 5‰ (excluding one distinct climate event that occurs at ~133.6±1.0 ka B.P.). We call this extended interval of time from 135.5±1.0 to 129.0±1.0 ka B.P. the "Weak Monsoon Interval" (WMI). This is a critical time interval in our record, as we are able to correlate this interval with events recorded in the Vostok ice core. This in turn yields clues about the sequence of events surrounding Termination II.

One of the most prominent, orbital-scale features of the monsoon $\delta^{18}O$ record over this time period is the abrupt shift towards more negative values at the start of the Last Interglacial Asian Monsoon. Precise ^{230}Th dating places the midpoint of this event, Asian Monsoon Termination II (AM TII), at 129.0±0.9 ka B.P., consistent with the value of Yuan et al. (2004). Yuan et al. (2004) constrained the length of this transition to < 200 years. At higher resolution, we show that the bulk of the transition (~1.7‰) between glacial and interglacial isotopic values occurred rapidly, in ~70 years. This presumes a constant growth rate across the $\delta^{18}O$ shift, which is bounded by ^{230}Th dates at 129.1±1.0 and 128.3±0.8 ka B.P. Though growth rate may vary between ^{230}Th-dated points, there is no indication that a significant change occurred during this time (Fig. 2a, top panel). Therefore, we estimate that AM TII was indeed a very rapid climatic transition, taking place on the order of 70 years.

The light $\delta^{18}O$ values characteristic of the Last Interglacial Asian Monsoon were sustained for the following 8.3±1.3 ky. Smaller amplitude variability is present in the Asian Monsoon $\delta^{18}O$ record during the Last Interglacial than during glacial times, though still significant (Fig. 6). $\delta^{18}O$ reaches values as light as − 9.5‰ in the well dated portion of sample D4. The lightest $\delta^{18}O$ values in sample D3 are similar, ~− 9.2‰. These values are comparable to the lightest $\delta^{18}O$ values seen during the Holocene (Dykoski et al., 2005). Over the entire Last Interglacial Period, $\delta^{18}O$ values generally vary between ~− 9.0‰ and ~− 8.0‰ in both samples D3 and D4.

The transition out of the Last Interglacial Asian Monsoon is marked by an increase in $\delta^{18}O$ values of 1.1‰ taking place in ~120-year period centered at 120.7±1.0 ka B.P. After this sharp transition, $\delta^{18}O$ values continued to gradually increase over the next several thousand years, for a total range of ~4‰. During the subsequent period of relatively weak monsoon (likely associated with MIS 5d), the heaviest $\delta^{18}O$ values are approximately − 4.7‰, comparable to the heaviest values during the MIS 6 glacial period. This is followed by a 3–4‰ shift towards more negative values, which appears as a double peak (likely associated with MIS 5c) that is approximately centered upon a peak in insolation. The first peak occurs at ~108 ka B.P. with a $\delta^{18}O$ value of − 9.0‰. By

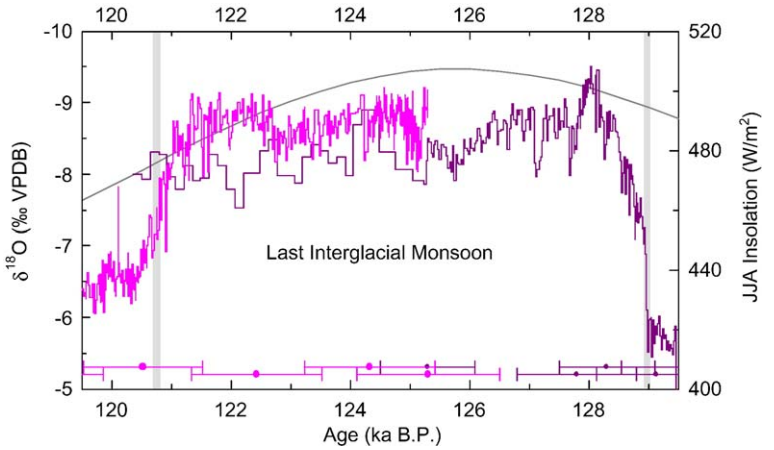

Fig. 6. The Last Interglacial Asian Monsoon $\delta^{18}O$ record from both speleothems D3 (pink) and D4 (purple). Vertical bars indicate the timing and duration of the transitions into (Asian Monsoon Termination II) and out of the Last Interglacial Asian Monsoon. Asian Monsoon Termination II occurred within 70 years at 129.0±0.8 ka BP, and the most abrupt portion of the transition out of the Last Interglacial Asian Monsoon (~ 120-year duration) is centered at 120.7±1.0 ka B.P. (For interpretation of the reference to colour in this figure legend, the reader is referred to the web version of this article.)

~105.2 ka B.P., $\delta^{18}O$ values were more than 2‰ heavier. $\delta^{18}O$ then returned to values around − 9.0‰ by ~105.0 ka B.P.

6. Discussion

6.1. Correlation strategy

Using our well-dated record of the Asian Monsoon, we are able to make global and regional correlations using several different strategies. We can directly compare our record to other absolute-dated climate records, such as other U-series dated speleothem records (Spötl et al., 2002; Bar-Matthews et al., 2003). Wang et al. (2001) demonstrated a strong correlation between the monsoon and Greenland temperature during deglacial times when the Greenland timescale is robust. On the basis of this relationship, they correlated events back to 75 ka B.P. by matching peaks. We have extended this correlation to older times using this strategy. We will also demonstrate that our record can be correlated to ice core records in both hemispheres using the atmospheric CH_4 record. The correlations to the Vostok record are particularly important as they allow us to determine a sequence of events during Termination II.

6.2. Insolation

Wang et al. (2001) and Yuan et al. (2004) have previously discussed the connection between the long term Hulu/Dongge Cave monsoon $\delta^{18}O$ record and Northern Hemisphere summer insolation (Berger, 1978). An increased amount of summer insolation is thought to enhance the thermal contrast between ocean and land, thereby intensifying the summer monsoon (Kutzbach, 1981). The structure of the Last Interglacial Asian Monsoon closely follows this insolation curve (Fig. 4), suggesting that AM TII was forced by insolation and may represent the final rise to full interglacial conditions. However, monsoon terminations are much more abrupt than the insolation curve. Rapid climate transitions such as this indicate that threshold effects internal to the climate system are likely involved (deMenocal et al., 2000; Yuan et al., 2004). A large shift in $\delta^{18}O$ also occurs at the 5d–5c transition, which also appears to be closely tied to insolation. The phasing of the shift may be slightly earlier relative to insolation than AM TII. It is plausible that the transition into the Last Interglacial Asian Monsoon lags insolation slightly due to the presence of larger ice sheets during the MIS 6 glacial.

6.3. MIS 6 "interstadials"

The Dongge Cave monsoon $\delta^{18}O$ record over late MIS 6 exhibits a series of sub-orbital scale climate events similar in magnitude to events recorded by Hulu Cave stalagmites (Wang et al., 2001) during the Last Glacial Period (Fig. 5). These "interstadial" events represent pluvial, or wet, periods in China, resulting from an intensification of the summer monsoon. Given that the errors associated with ^{230}Th ages at this time are on the order of ± 1000 years, it is difficult to quantify the

duration and frequency of these climate shifts. However, between 146 and 130 ka B.P. we identify 8 events with an amplitude ≥ 1‰. $\delta^{18}O$ amplitudes of these events average ~ 1.3‰, and the average time interval between peaks can be estimated to be ~ 1.8 ky. This is broadly similar to the millennial-scale events in the Hulu Cave record of the Last Glacial Period, though the Hulu record is also punctuated by heavy $\delta^{18}O$ excursions that are correlated with Heinrich events 1 to 6 in the North Atlantic (Bond et al., 1993; Wang et al., 2001). With the exception of our Weak Monsoon Interval (WMI) between 135.5 ± 1.0 and 129.0 ± 1.0 ka B.P., immediately prior to AM TII, extremely heavy $\delta^{18}O$ excursions do not appear to be as prominent in the portion of the Dongge Cave MIS 6 record studied here. North Atlantic sediment records indicate that at least one Heinrich event (H11) occurred during the penultimate glacial period, just before marine Termination II (McManus et al., 1998). Thus, our WMI likely correlates in some fashion with H11 in the North Atlantic.

6.4. Last Interglacial Asian Monsoon

A major issue is climate stability during interglacial periods. Whereas our record does not show evidence for instability with amplitudes as high as glacial–interglacial $\delta^{18}O$ shifts, there is clear evidence for abrupt, multi-decadal to centennial-scale shifts in $\delta^{18}O$ of up to ~ 1‰ during the Last Interglacial Asian Monsoon (Fig. 6). We have performed spectral analysis on the Dongge Cave $\delta^{18}O$ record of the Last Interglacial using the REDFIT program for unevenly spaced time series (Schulz and Mudelsee, 2002). Because of the slow growth rate in D4 after ~ 125 ka B.P., we analyzed only the older portion of the D4 Last Interglacial Asian Monsoon oxygen record. Between 128.2 and 125.3 ka B.P., the D4 $\delta^{18}O$ record has an average resolution of 23 years. We found a significant peak (above the 90% confidence level) at 111 years (Fig. 7a). Stalagmite D3 was used for analysis of the younger part of the Last Interglacial Asian Monsoon, between 121.0 ka B.P. and 125.3 ka B.P. (Fig. 7b). This portion of the record has a higher average resolution of 13 years, which allows higher frequency signals to be detected more accurately. We found a significant peak (above the 90% confidence level) at 119 years, similar to the 111-year peak seen in the D4 record. In addition, significant peaks are also found at 45, 42, 31, and 28 years. Comparable features with similar periodicities were found by Dykoski et al. (2005) during the Holocene in the younger portion of stalagmite D4 in the Dongge record. Our Last Interglacial shifts and Dykoski et al.'s Holocene shifts have amplitudes that are more than 1/2

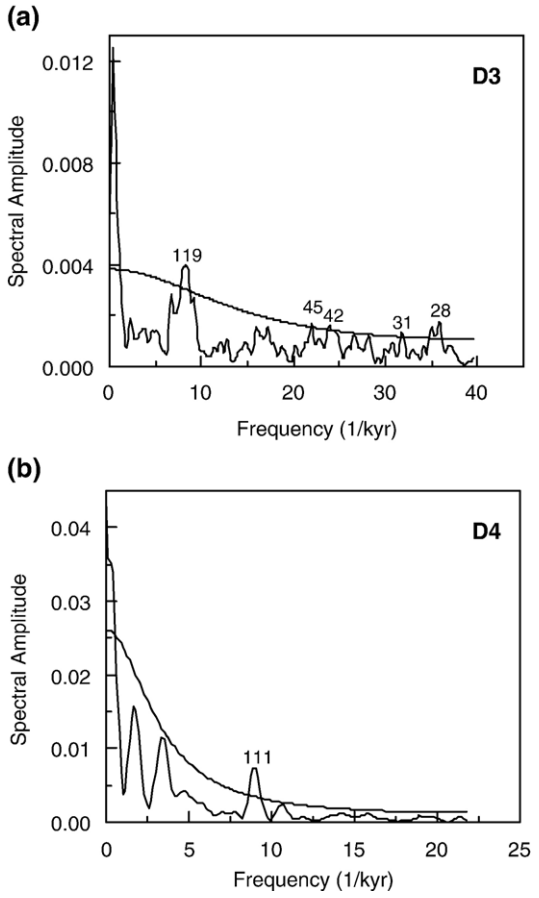

Fig. 7. Spectral analysis results for the Last Interglacial from (a) D3 (121.0 to 125.3 ka B.P.) and (b) D4 (128.2 to 125.2 ka B.P.). Results were obtained using the REDFIT spectral analysis program for unevenly spaced paleoclimate data (Schulz and Mudelsee, 2002). The spectra were calculated using the Welch-Overlapped-Segment-Averaging (WOSA) procedure, which divides the time series into n_{50} segments with 50% overlap and averages the results. 3 WOSA segments were used for the D3 time series, and 2 WOSA segments were used for the D4 time series. A Hanning spectral window was applied to each WOSA segment in order to reduce spectral leakage. Results were bias-corrected using 2000 Monte-Carlo simulations. Peaks above the 90% confidence level are labeled.

of the amplitude of millennial-scale events during the Last Glacial Period in China (Wang et al., 2001) and multi-centennial–millennial-scale events during MIS 6. It appears that abrupt climate changes are a general feature of interglacial periods, albeit with smaller amplitudes and generally higher frequency than events during glacial periods.

6.5. Greenland Interstadial Events

Correlation between the MIS 5 Dongge Cave record and the older portion of the Greenland ice core record of

$\delta^{18}O$ is also possible (GISP2 CD-ROM, 1997). Wang et al. (2001) previously demonstrated a connection between millennial-scale events from the MIS 2, 3, and 4 monsoon and Greenland Interstadial (GIS) events in the GISP2 record. Such events have been matched up from GIS 1 through GIS 21, which occurred at around 75 ka B.P. (Wang et al., 2001). A slightly revised correlation of GIS 19, 20, and 21 is shown in Fig. 8. Neither sample D3 nor D4 overlap with the Hulu samples at this time. The youngest part of speleothem D3 contains a double peak in $\delta^{18}O$ that correlates with the peak in insolation associated with MIS 5c. Although at somewhat lower resolution, a double peak feature similar to the Dongge record is also seen in speleothem records from Soreq and Peqiin Caves, Israel (Bar-Matthews et al., 2003). This double peak likely corresponds to Greenland Interstadials 23 and 24 during MIS 5c based on the correlation that has been made over the younger, more robust portion of the Greenland record (Fig. 8). If correct, peak to peak correlation would assign an age of 100.8±0.8 ka B.P. to GIS 23, and an age of 107.9±1.0 ka B.P. to GIS 24. There is new evidence from the NGRIP ice core that the oldest of the Greenland Interstadials, GIS 25, occurred sometime during or after the MIS 5e–5d transition (NGRIP Project Members, 2004). Though there appears to be some structure to the MIS 5d monsoon, we see no clear event that can be linked to GIS 25, the oldest of the Greenland Interstadials.

6.6. Termination II

There are conflicting theories regarding the timing, duration, and sequence of events leading up to the Last Interglacial Period. The $\delta^{18}O$ records from both Hulu and Dongge Caves follow Northern Hemisphere insolation over the last two glacial cycles, suggesting that insolation plays a strong part in forcing the Asian Monsoon (Wang et al., 2001; Yuan et al., 2004). However, a speleothem record from the Alps (Spötl et al., 2002), Devils Hole calcite (Winograd et al., 1997), Bahamian sediments (Henderson and Slowey, 2000), and Antarctic temperature and CO_2 records (Sowers et al., 1991; Broecker and Henderson, 1998; Petit et al., 1999) all suggest that warming at the MIS 6–5e boundary pre-dates the rise in insolation by several thousand years. This would indicate that a factor other than direct forcing by Northern Hemisphere summer insolation is controlling some aspect of glacial terminations. In the following discussion, Terminations I and II refer to the several thousand year periods surrounding the respective marine terminations, Greenland Termination I refers to the shift in $\delta^{18}O$ of ice prior to the Bølling-Allerød (B/A), Asian Monsoon Termination I

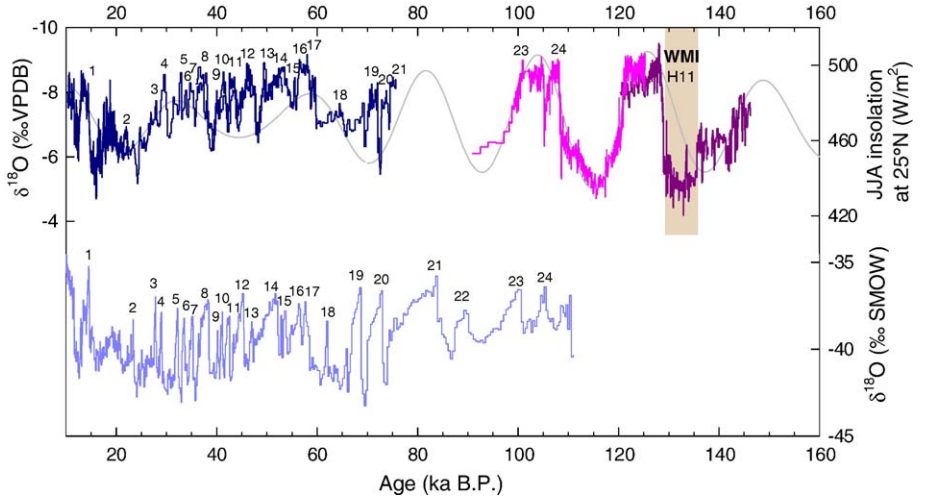

Fig. 8. $\delta^{18}O$ record of the Asian Monsoon over the last two glacial periods from Hulu (dark blue; Wang et al., 2001) and Dongge (purple; portion of record between 90 and 99 ka B.P. from Yuan et al., 2004) Caves, along with summer insolation at 25°N. Lower panel shows the GISP2 $\delta^{18}O$ record presented on the Meese/Sowers timescale (Meese et al., 1994). Data were obtained from the National Snow and Ice Data Center, University of Colorado at Boulder, and the World Data Center for Paleoclimatology, Boulder, Colorado (Greenland Summit Ice Cores [CD-ROM], 1997). Hulu Cave $\delta^{18}O$ peaks associated with Greenland Interstadial (GIS) events are labeled as in Wang et al. (2001), except for a slightly revised correlation of events 19–21. We have correlated the double peak feature in the youngest portion of the Dongge record with GIS 23 and 24, occurring at 100.8±0.8 and 107.9±1.0 ka B.P., respectively. (For interpretation of the reference to colour in this figure legend, the reader is referred to the web version of this article.)

(AM TI) describes the associated shift in monsoon $\delta^{18}O$, and AM TII is used as described above. We may be able to correlate changes in the monsoon with changes recorded in glacial ice through the atmospheric methane record, which has been linked to low latitude precipitation. If we are able to make monsoon–methane correlations near Termination II, it may be possible to address questions related to early climate amelioration at about this time.

Methane concentrations from both Northern and Southern Hemisphere ice cores demonstrate significant variability over glacial–interglacial cycles. The most important methane source contributing to these large fluctuations appears to be tropical and mid-high latitude wetlands (Fung et al., 1991; Chappellaz et al., 1993). Precipitation and temperature changes associated with glacial–interglacial transitions affect wetland extent and productivity, thus impacting the atmospheric methane signal. Chappellaz et al. (1990) found that the ice core CH_4 record has a strong precessional signal. Ruddiman and Raymo (2003) use this idea to make the argument that the methane signal is a response to the low-latitude monsoon, which was presumed to have a strong precessional component on the basis of its tie to insolation (Kutzbach, 1981). Evidence from a tropical lake core supports this idea, demonstrating the covariance between Vostok methane concentrations and humid/arid phases in the tropical desert region of Africa (Petit-Marie et al., 1991). In addition, over the last glacial cycle, interhemispheric methane gradient values were at their lowest during the B/A period just after Greenland Termination I (Brook et al., 2000). This supports the idea that the rise in methane concentrations at that time was dominated by a source increase in the tropics rather than the mid-high northern latitudes.

Our monsoon record (Wang et al., 2001; Yuan et al., 2004; and this work) provides strong support for a connection between monsoon intensity and atmospheric methane concentrations. There is a striking similarity between Hulu/Dongge $\delta^{18}O$ and the atmospheric methane record, a prime example of which is the portion of the record surrounding Termination I (Fig. 9a). The two records follow each other remarkably well over the transition into the B/A, the B/A, and the Younger Dryas. In fact, the monsoon $\delta^{18}O$ curve matches the methane record better than it matches the GISP2 oxygen record. However, immediately prior to AM TI, the relationship between the two records is not as strong, as methane concentrations began to increase at around 18 ka B.P. while the monsoon was still weak.

Based on the correlation seen during Termination I, we can look for a similar correlation around Termination II. Though CH_4 concentrations near Termination II begin to rise gradually along with CO_2 and temperature, there is indeed an abrupt final jump towards full interglacial concentrations (Fig. 9b). We correlate this abrupt CH_4 rise with AM TII. If this correlation is valid, the Petit et al. (1999) GT4 gas timescale is essentially accurate at this point in time as their placement of the abrupt CH_4 rise is approximately 129 ka B.P. Because of the close relationship between Greenland temperature and the Asian Monsoon (Wang et al., 2001), it is likely that temperature rise in Greenland was synchronous with AM TII. Thus, it appears that the initial phase of CH_4 rise and virtually all CO_2 and Vostok glacial–interglacial temperature rise preceded the abrupt increase in precipitation at AM TII as well as Greenland warming (Fig. 10). Prior to AM TII, we see an ~6 ky interval of heavy $\delta^{18}O$ values in our record that we have called the WMI. This period likely correlates with low Greenland temperatures and H11 in the North Atlantic, as discussed earlier. The CO_2 rise, Vostok temperature rise, and the gradual portion of the CH_4 rise occur almost entirely within this interval (Fig. 10a–d).

If the monsoon record is considered to be representative of climate in the Northern Hemisphere subtropics, we can conclude that this region was still experiencing dry, glacial conditions during the initial rise in CH_4 concentrations. On the basis of the relationship between the monsoon and Greenland temperatures, the high northern latitudes were also cold. The main source of methane at these times is therefore likely to have been from the tropics or the Southern Hemisphere. Speleothem evidence from semi-arid northeastern Brazil suggests that southern low to mid-latitudes were indeed relatively wet at this time. Wang et al. (2004) found that pluvial events, as indicated by speleothem growth periods, correspond to a weak Asian Monsoon, Heinrich events in the North Atlantic, and cold Greenland temperatures. Speleothem growth intervals occur just prior to both AM TI and TII (Fig. 9), suggesting that wet conditions existed in the southern low to mid-latitudes during the early phase of the atmospheric methane rise.

There is an extensive body of literature focusing on the rise in atmospheric CO_2 concentrations at glacial terminations. The challenge in uncovering the mechanism behind the deglacial CO_2 rise is that many models cannot explain both the long, gradual nature of the transition and the fact that it occurs early, prior to Northern Hemisphere climate change. However, the ocean is most certainly involved, since it is a large reservoir for CO_2. Martin (1990) proposed that higher CO_2 concentrations during interglacial periods result

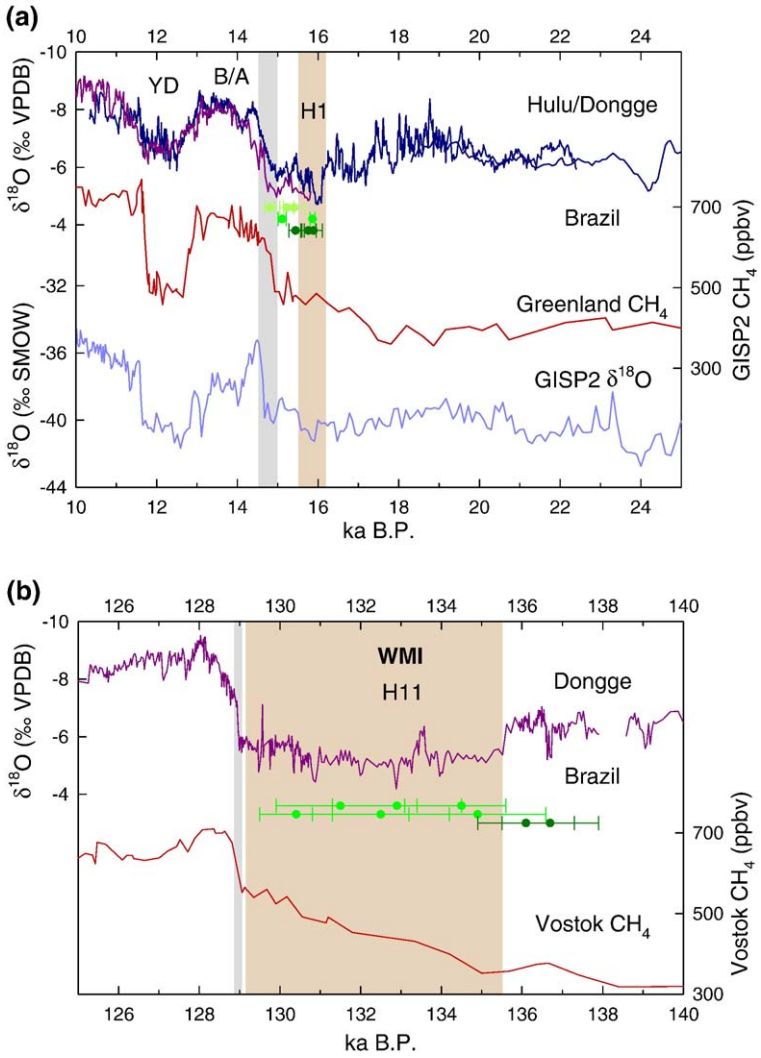

Fig. 9. (a) Hulu/Dongge $\delta^{18}O$ (Wang et al., 2001; Yuan et al., 2004; Dykoski et al., 2005; and this study), Greenland CH_4 (data from Brook et al., 2000; gas age timescale from Brook et al., 1996), and GISP2 $\delta^{18}O$ (Greenland Summit Ice Cores [CD-ROM], 1997) leading up to and following the most recent deglaciation. H1 and Asian Monsoon Termination I are indicated by vertical bars, and the Bølling-Allerød and Younger Dryas periods are labeled. There is an error in the relationship between $\delta^{18}O$ of ice and CH_4 of ~ 350 years at this time due to the gas–ice age conversion (Brook et al., 1996). (b) Dongge Cave $\delta^{18}O$ from stalagmite D4 during the Penultimate Glacial Period and deglaciation compared to Vostok CH_4 (Petit et al., 1999). Vertical bars indicate the WMI/H11 and Asian Monsoon Termination II. Speleothem growth intervals from northeastern Brazil (Wang et al., 2004) are designated by separated dots with 2σ error bars (in different shades for different samples).

from limitations in oceanic productivity and CO_2 drawdown due to an iron deficiency. This is a plausible model because during glacial times, there is an increased supply of Fe-bearing dust to the Southern Ocean and Antarctic ice cores, the source of which is thought to be Patagonia (e.g. Grousset et al., 1992). Vostok dust supply decreases prior to the increase in atmospheric CO_2 concentration (Fig. 10f). Broecker and Henderson (1998) suggest the additional involvement of nitrogen fixation, with the long oceanic residence time of nitrate necessary to modulate the gradual atmospheric CO_2 rise. Whether or not nitrogen fixation is a factor in the CO_2 rise, the iron fertilization model broadly fits the sequence of events outlined here, as warm, wet conditions in the southern low to mid-latitudes during the WMI would contribute to a low dust flux to Antarctica and the Southern Ocean as observed (Fig. 10).

Within error, Southern Hemisphere warming at Vostok coincides with the rise in CO_2, so it is plausible that the CO_2 rise contributes to the Vostok temperature rise, although potential lead/lag and cause/effect

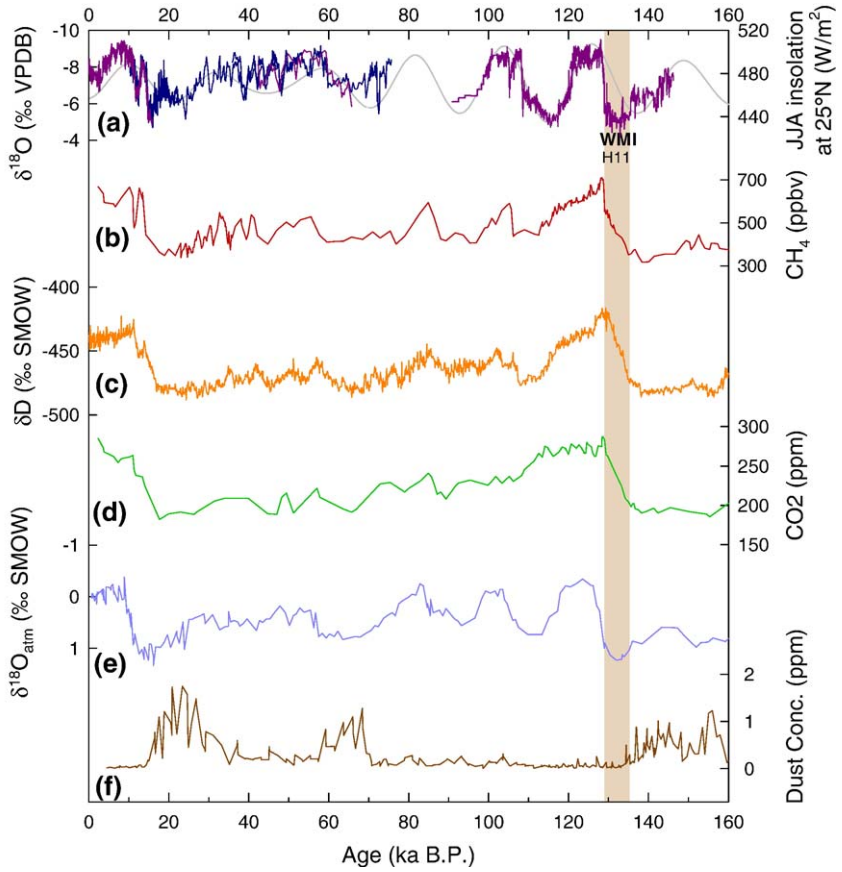

Fig. 10. Comparison of (a) Hulu/Dongge $\delta^{18}O$ (Wang et al., 2001; Yuan et al., 2004; Dykoski et al., 2005; and this study) with Vostok ice core records of (b) CH_4, (c) δD (a proxy for temperature), (d) CO_2, (e) $\delta^{18}O_{atm}$, and (f) dust concentration between 0 and 160 ka B.P. (Petit et al., 1999). The vertical bar indicates the WMI/H11. We correlate Asian Monsoon Termination II to the abrupt jump in CH_4 concentrations at ~ 129 ka B.P. (see Fig. 8b).

relationships are unclear (see Barnola et al., 1991 for a general discussion, and Caillon et al., 2003 for a discussion of Termination III). On the other hand, the CO_2 rise occurs during our WMI, likely an extended cold interval in the northern high latitudes. Thus, any global increase in heat associated with rising atmospheric CO_2 is reflected in the Southern, but not Northern, Hemisphere temperature rise. The "bipolar seesaw" hypothesis has been invoked to explain asynchronous climate change between hemispheres (Broecker, 1998; Blunier et al., 1998; Blunier and Brook, 2001). Examples of the phase of the bipolar seesaw, characterized by the alternation of enhanced deep water formation and transport of heat between the Southern Ocean and the North Atlantic, include early southern warming during Termination I (Broecker, 1998) and Last Glacial Period Heinrich events (Blunier and Brook, 2001). Our WMI may correspond qualitatively to events such as these, but with much larger duration and amplitude. As qualitatively similar (although different magnitude) southern heating events preceded both AM TI and TII and associated Greenland warming, it appears that these events are an important aspect of glacial terminations.

6.7. Sea level

A reliable record of sea level across the Penultimate Glacial/Last Interglacial time interval is critical to understanding global and regional climatic connections involved in glacial terminations. Sea level has been determined for this time period by dating of coral terraces (Stein et al., 1993; Gallup et al., 2002). The final rise to interglacial values is synchronous within error with AM TII. Yet sea level rose to within 18±3 m of present sea level by 135.8±0.8 ka B.P., prior to the rise in insolation. U–Th isochron dating of aragonite-rich sediments from the Bahamas yields an age for the midpoint of the transition into the Last Interglacial of 135±2.5 ka (Henderson and Slowey, 2000). Though it

is not a direct measure of sea level, this date is consistent with sea level estimates of deglacial timing. This implies that another mechanism must have been responsible for driving sea level changes at that time.

$\delta^{18}O_{atm}$ is also considered a proxy for global ice volume, as variability in the $\delta^{18}O$ of seawater is the main factor influencing the $\delta^{18}O$ of O_2 (Sowers et al., 1991; Sowers et al., 1993; Bender et al., 1994b). Changes $\delta^{18}O_{atm}$ should lag sea level by ~1–2 ky based on the turnover rate of O_2 in the atmosphere (Bender et al., 1994a). If our monsoon methane correlation is correct, the half height of the rise in $\delta^{18}O_{atm}$ at the end of the Penultimate Glacial Period is at precisely 128 ka B.P. (Fig. 10e), suggesting that the half height of the deglacial sea level rise occurred at ~130 ka B.P. If previous estimates of early sea level rise are correct (at ~135 ka B.P., Stein et al., 1993; Henderson and Slowey, 2000; Gallup et al., 2002), it would either suggest that $\delta^{18}O_{atm}$ is not an accurate proxy for global ice volume, or our monsoon–methane correlation is incorrect. However, some question remains as to the stratigraphy of the Barbados coral terrace (Gallup et al., 2002). Resolution of the timing of sea level rise would be important to our understanding of the sequence of events surrounding glacial terminations.

6.8. The Alps

Warming at ~135 ka is also implied by several terrestrial records, including pollen records, speleothem deposition, benthic shelf foraminifera, and pedogenic stratigraphy (Seidenkrantz et al., 1996; Spötl et al., 2002). One such record is from Spannagel Cave, located in the Austrian Alps (Spötl et al., 2002). This cave is proximal to alpine glaciers in today's climate, and during glacial periods the ice moved over the cave region. Deposition of calcite is not possible if glacial ice or permafrost overlay the cave. Therefore, periods of speleothem deposition represent ice-free conditions in the Austrian Alps. U-series dating of a flowstone from this cave show an interval of speleothem growth beginning at 135±1.2 ka, indicating that warm conditions existed at this time, prior to AM TII.

The Dongge Cave $\delta^{18}O$ record demonstrates that AM TII occurred at 129.0±0.9 ka B.P. and that the monsoon was generally weak for several millennia (~136 to ~130 ka B.P.) prior to the Monsoon Termination. To the extent that millennial-scale events in China correlate with analogs in Greenland, it is likely that this weak interval corresponds with cold North Atlantic/European climate. If so, the Alps speleothem growth event likely correlates with the end of the last interstadial event prior to this weak monsoon interval. The end of this interstadial event is at 135.5±1.0 ka B.P., within error of the Alps growth interval. Alternately, the weak monsoon interval is punctuated by a distinct climatic event at 133.6±1.0 ka B.P., also within error of the Alps event (Fig. 5). A warm interstadial-type event such as this could serve as an alternate correlation to the Alps warming at this time.

7. Conclusions

The history and variability of the Asian Monsoon has been studied using the $\delta^{18}O$ record of speleothems from Hulu and Dongge Caves. New high resolution data confirms that Asian Monsoon Termination II (AM TII) was an abrupt climate event that occurred in the D4 $\delta^{18}O$ record at 129.0±0.8 ka B.P. The bulk of this transition took place in 70 years. The sharpest drop in $\delta^{18}O$ values during the transition out of this warm period (1.1‰) occurred in ~120 years, and is centered at 120.7±1.0 ka B.P. The Asian Monsoon does appear to be forced by Northern Hemisphere summer insolation at 25°N, though the monsoon record is punctuated by sharp transitions into and out of glacial periods and multi-decadal to millennial-scale climate shifts. This suggests the involvement of some sort of threshold effect. AM TII may mark the final rise to full interglacial conditions.

We have extended Wang et al.'s (2001) monsoon–Greenland correlation to include GIS events 23 and 24, which we correlate with a double peak feature between ~110 and 100 ka B.P. in the Dongge Cave monsoon record. This feature is similar to a double peak feature seen in speleothem records from Soreq and Peqiin Cave, Israel (Bar-Matthews et al., 2003). Significant variability exists over the entire monsoon record, during both glacial and interglacial periods. Millennial-scale climate events during the last portion MIS 6 average 1.3‰ in amplitude and have an average frequency of 1.8 ky. This is broadly similar to the millennial-scale events in the Hulu Cave $\delta^{18}O$ record of the Last Glacial Period. The Last Interglacial Asian Monsoon $\delta^{18}O$ record has significant variability with multi-decadal to multi-centennial-scale events with amplitudes of up to 1‰, more than half the amplitude of glacial interstadial events. Last Interglacial variability is similar to the Holocene in terms of frequency and magnitude (Dykoski et al., 2005), indicating that significant monsoon variability is a general feature of interglacial climate. An extended interval of heavy $\delta^{18}O$ values is observed during the Penultimate Glacial Period between 135.5±1.0 and 129.0±1.0 ka B.P., immediately prior to

AM TII. We correlate this Weak Monsoon Interval (WMI) with H11 and low temperatures in Greenland.

The monsoon record broadly follows atmospheric CH_4 concentrations over the last two glacial cycles. This relationship is particularly impressive during and after the transition into the Bølling-Allerød. We found a similar relationship around Termination II, and correlate the abrupt jump in CH_4 concentrations at this time with our Asian Monsoon Termination II. Based upon this correlation, we show that the full Termination II atmospheric CO_2 and Antarctic temperature rise, and the gradual portion of the CH_4 rise occur almost entirely within the WMI. Therefore, we infer that atmospheric CO_2, Antarctic temperature, and the initial portion of the CH_4 rise preceded the increase in monsoon precipitation and warming in Greenland. Early Southern Hemisphere warming during Termination I and Last Glacial Period Heinrich events has been attributed to the "bipolar seesaw" mechanism (Broecker, 1998; Blunier et al., 1998; Blunier and Brook, 2001). The WMI is qualitatively similar (though different in magnitude) to these Heinrich events, so it appears as though early southern warming events are an important aspect of glacial terminations. We suggest that the "bipolar seesaw" mechanism may contribute to the sequence of events surrounding glacial terminations.

Acknowledgements

We would like to thank Gary Comer and Wally Broecker for their strong and generous support of our work and Maniko Solheid for performing stable isotope analyses. We also thank Gideon Henderson and one anonymous reviewer for their helpful reviews of this manuscript. This work was supported by NSF Grants 0214041 and 0116395, CNSF Grant 40328005, NSF Grant 0502535, and Gary Comer Science and Education Foundation Grant CC8. All data from this paper are available from the World Data Center for Paleoclimatology at http://www.ncdc.noaa.gov/paleo/speleothem.html.

References

Ayliffe, L.K., Veeh, H.H., 1988. Uranium-series dating of speleothems and bones from Victoria Cave, Naracoorte, Australia. Chemical Geology 72, 211–234.

Baker, A., Barnes, W.L., Smart, P.L., 1997. Variations in the discharge and organic matter content of stalagmite drip waters in Lower Cave, Bristol. Hydrological Processes 11, 1541–1555.

Baker, A., Genty, D., Dreybrodt, W., Barnes, W.L., Mockler, N.J., Grapes, J., 1998. Testing theoretically predicted stalagmite growth rate with recent annually laminated samples: implications for past stalagmite deposition. Geochimica et Cosmochimica Acta 62, 393–404.

Bard, E., Antonioli, F., Silenzi, S., 2002. Sea level during the penultimate glacial period based on a submerged stalagmite from Argentarola Cave (Italy). Earth and Planetary Science Letters 196, 135–146.

Bar-Matthews, M., Ayalon, A., Gilmour, M., Matthews, A., Hawkesworth, C.J., 2003. Sea–land oxygen isotopic relationships from planktonic foraminifera and speleothems in the Eastern Mediterranean region and their implication for paleorainfall during interglacial intervals. Geochimica et Cosmochimica Acta 67, 3181–3199.

Barnola, J.-M., Pimienta, P., Raynaud, D., Korotkevich, Y.S., 1991. CO_2–climate relationship as deduced from the Vostok ice core: a re-examination based on new measurements and on a re-evaluation of the air dating. Tellus 43B, 83–90.

Bender, M., Sowers, T., Labeyrie, L., 1994a. The Dole effect and its variations during the last 130,000 years as measured in the Vostok ice core. Global Biogeochemical Cycles 8, 363–376.

Bender, M., Sowers, T., Dickson, M.-L., Orchardo, J., Grootes, P., Mayewski, P.A., Meese, D.A., 1994b. Climate correlations between Greenland and Antarctica during the past 100,000 years. Nature 372, 663–669.

Berger, A.L., 1978. Long-term variations of caloric insolation resulting from the Earth's orbital elements. Quaternary Research 9, 139–167.

Blunier, T., Brook, E.J., 2001. Timing of millennial-scale climate change in Antarctica and Greenland during the Last Glacial Period. Science 291, 109–112.

Blunier, T., Chappellaz, J., Schwander, A., Dallenbach, A., Stauffer, B., Stocker, T.F., Raynaud, D., Jouzel, J., Clausen, H.B., Hammer, C.U., Johnsen, S.J., 1998. Asynchrony of Antarctic and Greenland climate change during the last glacial period. Nature 394, 739–743.

Bond, G., Broecker, W., Johnson, S., McManus, J., Labeyrie, L., Jouzel, J., Bonani, G., 1993. Correlations between climate records from North Atlantic sediments and Greenland ice. Nature 365, 143–147.

Broecker, W.S., 1998. Paleocean circulation during the last deglaciation: a bipolar seesaw? Paleoceanography 13, 119–121.

Broecker, W.S., Henderson, G.M., 1998. The sequence of events surrounding Termination II and their implications for the cause of glacial–interglacial CO_2 changes. Paleoceanography 13, 264–352.

Brook, E.J., Sowers, T., Orchardo, J., 1996. Rapid variations in atmospheric methane concentration during the past 110,000 years. Science 273, 1087–1091.

Brook, E.J., Harder, S., Severinghaus, J., Steig, E.J., Sucher, C.M., 2000. On the origin and timing of rapid changes in atmospheric methane during the last glacial period. Global Biogeochemical Cycles 14, 559–572.

Caillon, N., Severinghaus, J.P., Jouzel, J., Barnola, J.-M., Kang, J., Lipenkov, V.Y., 2003. Timing of atmospheric CO_2 and Antarctic temperature changes across Termination III. Science 299, 1728–1731.

Chappellaz, J., Barnola, J.M., Raynaud, D., Korotkevich, Y.S., Lorius, C., 1990. Ice-core record of atmospheric methane over the past 160,000 years. Nature 345, 127–131.

Chappellaz, J.A., Fung, I.Y., Thompson, A.M., 1993. The atmospheric CH_4 increase since the Last Glacial Maximum. Tellus 45B, 228–241.

Criss, R.E., 1999. Principles of Stable Isotope Distribution. Oxford University Press, New York, NY.

Dansgaard, W., 1964. Stable isotope in precipitation. Tellus XVI, 436–468.

deMenocal, P., Ortiz, J., Guilderson, T., Adkins, J., Sarnthein, M., Baker, L., Yarusinsky, M., 2000. Abrupt onset and termination of the African Humid Period: rapid climate responses to gradual insolation forcing. Quaternary Science Reviews 19, 347–361.

Dorale, J.A., Edwards, R.L., Ito, E., Gonzalez, L.A., 1998. Climate and vegetation history of the midcontinent from 75 to 25 ka: a speleothem record from Crevice Cave, Missouri, USA. Science 282, 1871–1874.

Dorale, J.A., Edwards, R.L., Alexander, E.C., Shen, C.-C., Richards, D.A., Cheng, H., 2005. U-series dating of speleothems: techniques, limits, and applications. In: Sasowsky, I.D., Mylroic, J.E. (Eds.), Studies of Cave Sediments. Kluwer Academic/Plenum Publishers, New York, pp. 177–197.

Dreybrodt, W., 1980. Deposition of calcite from thin films of natural calcareous solutions and the growth of speleothems. Chemical Geology 29, 80–105.

Dykoski, C.A., Edwards, R.L., Cheng, H., Yuan, D., Cai, Y., Zhang, M., Lin, Y., An, Z., Revenaugh, J., 2005. A high resolution, absolute-dated Holocene and deglacial Asian monsoon record from Dongge Cave, China. Earth and Planetary Science Letters 233, 71–86.

Edwards, R.L., Chen, J.H., Wasserburg, G.J., 1987. ^{238}U–^{234}U–^{230}Th–^{232}Th systematics and the precise measurement of time over the past 500,000 years. Earth and Planetary Science Letters 81, 175–192.

Friedman, I., O'Neil, J.R., 1977. Compilation of stable isotope fractionation factors of geochemical interest. U.S. Geological Survey Professional Paper 440-KK.

Fung, I., John, J., Lerner, J., Matthews, E., Prather, M., Steele, L.P., Fraser, P.J., 1991. Three-dimensional model synthesis of the global methane cycle. Journal of Geophysical Research 96, 13,033–13,065.

Gallup, C.D., Cheng, H., Taylor, F.W., Edwards, R.L., 2002. Direct determination of the timing of sea level change during Termination II. Science 295, 310–313.

Genty, D., Quinif, Y., 1996. Annually laminated sequences in the internal structure of some Belgian stalagmites—importance for paleoclimatology. Journal of Sedimentary Research 66, 275–288.

Gomez, R., Gonzalez, L.A., Cheng, H., Edwards, R.L., Urbani, F., 2003. Late glacial stage–Holocene transition recorded in a northern South American stalagmite. GSA Abstracts with Programs, Seattle Annual Meeting.

Greenland Summit Ice Cores [CD-ROM], 1997. National Snow and Ice Data Center, University of Colorado at Boulder, and the World Data Center for Paleoclimatology, Boulder, Colorado.

Grousset, F.E., Biscaye, P.E., Revel, M., Petit, J.-R., Pye, K., Joussaume, S., Jouzel, J., 1992. Antarctic (Dome C) ice-core dust at 18 k.y. B.P.: isotopic constraints on origins. Earth and Planetary Science Letters 111, 175–182.

Hellstrom, J.C., McCulloch, M.T., 2000. Multi-proxy constraints on the climatic significance of trace element records from a New Zealand speleothem. Earth and Planetary Science Letters 179, 287–297.

Henderson, G.M., Slowey, N.C., 2000. Evidence from U–Th dating against Northern Hemisphere forcing of the penultimate deglaciation. Nature 404, 61–66.

Henderson, G.M., Slowey, N.C., Haddad, G.A., 1999. Fluid flow through carbonate platforms: constraints from $^{234}U/^{238}$ and Cl^{-} in Bahamas pore-waters. Earth and Planetary Science Letters 169, 99–111.

Hendy, C.H., 1971. The isotope geochemistry of speleothems: I. The calculation of the effects of different modes of formation on the isotopic composition of speleothems and their applicability as paleoclimatic indicators. Geochimica et Cosmochimica Acta 35, 801–824.

IAEA/WMO, 2001. Global Network of Isotopes in Precipitation. The GNIP Database. Accessible at: http://isohis.iaea.org.

Johnson, K.R., Ingram, B.L., 2004. Spatial and temporal variability in the stable isotope systematics of modern precipitation in China: implications for paleoclimate reconstructions. Earth and Planetary Science Letters 220, 365–378.

Jouzel, J., Koster, R.D., Suozzo, R.J., Russell, G.L., 1994. Stable water isotope behavior during the last glacial maximum: a general circulation model analysis. Journal of Geophysical Research 99, 25,791–725,801.

Kaufman, A., Wasserburg, G.J., Porcelli, D., Bar-Matthews, M., Ayalon, A., Halicz, L., 1998. U–Th isotope systematics from the Soreq cave, Israel and climatic correlations. Earth and Planetary Science Letters 156, 141–155.

Kutzbach, J.E., 1981. Monsoon climate of the early Holocene: climate experiment with the Earth's early orbital parameters for 9000 years ago. Science 214, 59–61.

Martin, J.H., 1990. Glacial–interglacial CO_2 change: the iron hypothesis. Paleoceanography 5, 1–13.

McManus, J.F., Anderson, R.F., Broecker, W.S., Fleisher, M.Q., Higgins, S.M., 1998. Radiometrically determined sedimentary fluxes in the sub-polar North Atlantic during the last 140,000 years. Earth and Planetary Science Letters 155, 29–43.

Meese, D.A., Alley, R.B., Fiacco, R.J., Germani, M.S., Gow, A.J., Grootes, P.M., Illing, M., Mayewski, P.A., Morrison, M.C., Ram, M., Taylor, K.C., Yang, Q., Zielinki, G.A., 1994. Preliminary depth–agescale of the GISP2 ice core. CRREL Special Report 94-1.

Musgrove, M., Banner, J.L., Mack, L.E., Combs, D.M., James, E.W., Cheng, H., Edwards, R.L., 2001. Geochronology of late Pleistocene to Holocene speleothems from central Texas; implications for regional paleoclimate. Geological Society of America Bulletin 113, 1532–1543.

North Greenland Ice Core Project Members, 2004. High-resolution record of Northern Hemisphere climate extending into the last interglacial period. Nature 431, 147–151.

Osmond, J.K., 1980. Uranium disequilibrium in hydrologic studies. In: Fritz, P., Fontes, J.C. (Eds.), Handbook of Environmental Geochemistry, vol. 1. Elsevier, Amsterdam, pp. 259–282.

Osmond, J.K., Cowart, J.B., 1982. Groundwater. In: Ivanovich, M., Harmon, R.S. (Eds.), Uranium Series Disequilibrium: Applications to Environmental Problems. Oxford University Press, New York, pp. 202–245.

Petit, J.R., Jouzel, J., Raynaud, D., Barkov, N.I., Barnola, J.-M., Basile, I., Bender, M., Chappellaz, J., Davis, M., Delaygue, G., Delmotte, M., Kotlyakov, V.M., Legrand, M., Lipenkov, V.Y., Lorius, C., Pepin, L., Ritz, C., Saltzman, E., Stievenard, M., 1999. Climate and atmospheric history of the past 420,000 years from the Vostok ice core, Antarctica. Nature 399, 429–436.

Petit-Marie, N., Fontugne, M., Rouland, C., 1991. Atmospheric methane ratio and environmental changes in the Sahara and Sahel during the last 130 kyrs. Palaeogeography, Palaeoclimatology, Palaeoecology 86, 197–204.

Rosholt, J.N., Doe, B.R., T., M., 1966. Evolution of the isotopic composition of uranium and thorium in soil profiles. Geological Society of America Bulletin 77, 987–1004.

Rozanski, K., Araguas-Araguas, L., Gonfiantini, R., 1993. Isotopic patterns in modern global precipitation. In: Swart, P.K., Lohmann,

J., McKenzie, J., Savin, S. (Eds.), Geophysical Monograph, vol. 78. American Geophysical Union, pp. 1–36.

Ruddiman, W.F., Raymo, M.E., 2003. A methane-based time scale for Vostok ice. Quaternary Science Reviews 22, 141–155.

Schulz, M., Mudelsee, M., 2002. REDFIT: estimating red-noise spectra directly from unevenly spaced paleoclimatic time series. Computers & Geosciences 28, 421–426.

Seidenkrantz, M.-S., Bornmalm, L., Johnsen, S.J., Knudsen, K.L., Kuijpers, A., Lauritzen, S.-E., Leroy, S.A.G., Mergeal, I., Schweger, C., Van Vliet-Lanoe, B., 1996. Two-step deglaciation at the oxygen isotope stage 6/5e transition: the Zeifen-Kattegat climate oscillation. Quaternary Science Reviews 15, 63–75.

Shen, C.-C., Edwards, R.L., Cheng, H., Dorale, J.A., Thomas, R.B., Moran, S.B., Weinstein, S., Hirschmann, M., 2002. Uranium and thorium isotopic and concentration measurements by magnetic sector inductively coup led plasma mass spectrometry. Chemical Geology 185, 165–178.

Sowers, T., Bender, M., Raynaud, D., Korotkevich, Y.S., Orchardo, J., 1991. The $\delta^{18}O$ of atmospheric O_2 from air inclusions in the Vostok ice core: timing of CO_2 and ice volume changes during the penultimate deglaciation. Paleoceanography 6, 679–696.

Sowers, T., Bender, M., Labeyrie, L., Martinson, D., Jouzel, J., Raynaud, D., Pichon, J.J., Korotkevich, Y.S., 1993. A 135,000-year Vostok-SPECMAP common temporal framework. Paleoceanography 8, 737–766.

Spötl, C., Mangini, A., Frank, N., Eichstadter, R., Burns, S.J., 2002. Start of the last interglacial period at 135 ka: evidence from a high Alpine speleothem. Geology 30, 815–818.

Stein, M., Wasserburg, G.J., Aharon, P., Chen, J.H., Zhu, Z.R., Bloom, A., Chappell, J., 1993. TIMS U-series dating and stable isotopes of the last interglacial event in Papua New Guinea. Geochimica et Cosmochimica Acta 57, 2541–2554.

Stirling, C.H., Lee, D.-C., Christensen, J.N., Halliday, A.N., 2000. High-precision in situ ^{238}U–^{234}U–^{230}Th isotopic analysis using laser ablation multiple-collector ICPMS. Geochimica et Cosmochimica Acta 64, 3737–3750.

Wang, Y.J., Cheng, H., Edwards, R.L., An, Z.S., Wu, J.Y., Shen, C.-C., Dorale, J.A., 2001. A high-resolution absolute-dated Late Pleistocene monsoon record from Hulu Cave, China. Science 294, 2345–2348.

Wang, X., Auler, A.S., Edwards, R.L., Cheng, H., Cristalli, P.S., Smart, P.L., Richards, D.A., Shen, C.-C., 2004. Wet periods in northeastern Brazil over the past 210 kyr linked to distant climate anomalies. Nature 432, 740–743.

Winograd, I.J., Landwehr, J.M., Ludwig, K.R., Coplen, T.B., Riggs, A. C., 1997. Duration and structure of the past four interglaciations. Quaternary Research 48, 141–154.

Yuan, D., Cheng, H., Edwards, R.L., Dykoski, C.A., Kelly, M.J., Zhang, M., Qing, J., Lin, Y., Wang, Y., Wu, J., Dorale, J.A., An, Z., Cai, Y., 2004. Timing, duration, and transitions of the Last Interglacial Asian Monsoon. Science 304, 575–578.